Bioelectrochemical profiling of two common polymorphic variants of human FMO3 in presence of graphene oxide

Bioelectrochemical profiling of two common polymorphic variants of human FMO3 in presence of graphene oxide

Silvia Castrignanò[a], Stefania Bortolussi[a], Gianluca Catucci[a], Omkolsum Gholami[a], Francesca Valetti[a], Gianfranco Gilardi[a,b], Sheila J. Sadeghi[a,b]*

[a]Department of Life Sciences and Systems Biology, University of Torino, Italy.

[b]Centre for Nanostructured Interfaces and Surfaces, University of Torino, Italy.

CORRESPONDING AUTHOR

*Sheila Sadeghi, Department of Life Sciences and Systems Biology, Via Accademia Albertina 13, 10123 Turin, Italy. Phone: +39-011-6704528, Fax: +39-011-6704643, E-mail: sheila.sadeghi@unito.it

Abstract

Genetic variation of phase I drug metabolising enzymes demonstrated to greatly influence inter-individual reaction to pharmacological treatments. Among these enzymes, human flavin-containing monooxygenase 3 (hFMO3) plays a crucial role and understanding its pharmacogenetics is fundamental for the prediction of individual drug response and the efficacy of therapy. In this work the altered drug metabolism of two common polymorphic variants of hFMO3 (E158K and E308G) are studied by using an electrochemical platform modified with graphene oxide (GO). Electrochemistry was used to characterise the properties of these two engineered and purified hFMO3 variants followed by electrocatalysis experiments in the presence of three different hFMO3 substrates benzydamine, tamoxifen and sulindac sulfide. HPLC quantification of the electrochemically produced metabolites showed that E158K mutation leads to an impairment of N-oxygenation activity while E308G mutation enhances the same activity.

Results demonstrate that electrocatalysis on GO modified glassy carbon electrodes provides a fast and reliable method for measuring kinetic parameters of hFMO3 polymorphic variants. This method can be considered suitable for deciphering metabolic implications of polymorphisms that might lead to adjustment of drug dosages depending on the individual's genetic makeup, a step closer to the development of personalised medicine.

Keywords

flavin-containing monooxygenase, glassy carbon electrode, graphene oxide, electrocatalysis, FTIR, personalized medicine.

1. Introduction

Drug metabolising enzymes are highly involved in the metabolism of potentially dangerous foreign chemicals into less harmful and more readily excretable molecules in humans. Among these enzymes, human flavin-containing monooxygenase isoform 3 (hFMO3) is able to catalyse the oxygenation of a variety of xenobiotics with varied chemical structures, including many therapeutic drugs [1]. This enzyme is microsomal, FAD- and NADPH-dependent and, is able to activate molecular oxygen to catalyse substrate oxygenation [1-3,4]. Recently, in addition to xenobiotic metabolism, FMO3 has also been implicated in the development of atherosclerosis, cholesterol imbalance and to glucose and lipid metabolism [5-7]. Human FMO3 activity is widely recognized as being part of the first-pass metabolism of drugs together with the superfamily of cytochrome P450 enzymes [1]. Differently to cytochromes P450, hFMO3 metabolism is responsible for the polarization of drugs and xenobiotic molecules that are consequently converted into more excretable species so hFMO3 activity has clinical relevance in the detoxification and clearance processes. Therefore, the development of new chemical entities that can be metabolized by hFMO3 rather cytochromes P450, can decrease the toxic side effects and be more tolerable by patients. In addition, while cytochromes P450 can be readily induced or inhibited with high probability of adverse drug-drug interactions, hFMO3 activity has not been shown to be influenced by foreign chemical species [1].

The natural polymorphism of FMO enzymes has been shown to strongly influence inter-individual drug response increasing the significance of these enzymes from a pharmacological as well as toxicological point of view [7,8]. Human FMO3 is a highly polymorphic enzyme and many of its single nucleotide polymorphisms are present at reasonably high frequency within the population [9]. *In vivo* studies of the metabolism of drugs such as benzydamine, tamoxifen and sulindac sulfide, have demonstrated a strict relationship between some common hFMO3 nucleotide polymorphisms and their altered metabolism. It has also been demonstrated

that simultaneous occurrence, like in the case of the two common polymorphic variants E158K and E308G, leads to a significant alteration in hFMO3 metabolism [10]. Furthermore, mutations leading to the total loss of hFMO3 function are the genetic basis for the trimethymaminuria disease [11,12]. People affected by this disease are not able to metabolize the odorous trimethylamine to its odourless N-oxide and the accumulated trimethylamine leads to the so-called fish-odour syndrome [13].

For these reasons, the understanding of hFMO3 pharmacogenetics would be fundamental in the prediction of individual drug response and therapy efficacy leading to a major contribution to drug design and development [9]. In light of this, much attention has been concentrated on the development of new methods useful for pharmacological research relevant to hFMO3 catalysis. One such technique which is applicable to these enzymes is electrochemistry where the direct electrochemical response of hFMO3 on gold and carbon surfaces has been previously demonstrated by our group [14-16]. The advantage of direct immobilization of hFMO3 on electrode surface is mostly related to the possibility of using reducing equivalents provided by the electrode surface instead of those of NADPH which is its natural redox partner, thus improving experimental conditions in terms of costs, reliability and efficiency. To further enhance the electrochemical response of this enzyme novel material such as graphene and/or graphene oxide (GO) can be employed [18]. GO has been found to have applications in a variety of new applications such as electronic devices, sensors and energy-related techniques due to its interesting properties. The presence of oxygen functionalities causes a decrease of GO conductivity but, on the other hand, it improves GO solubility in aqueous solutions and allows the interaction with a number of chemical entities. Moreover, water solubility is consistent with the higher biological compatibility of GO compared to graphene that needs to be properly supported in order to be able to interact with biological substrates [19,20]. These peculiar characteristics have been considered promising for the development of a variety of

biosensing strategies in which graphene material has been applied as a transducer of biological signals in electrochemical, fluorescence and impedance biosensors [21-24].

Here, we report the extension of the GO-based electrochemical approach [21] to two common polymorphic variants of hFMO3 enzyme, E158K and E308G. These two hFMO3 variants were expressed in a recombinant system and immobilised on didodecyldimethylammonium bromide (DDAB)/GO glassy carbon electrodes and their activity tested with three hFMO3 marker drugs: benzydamine, a non-steroidal anti-inflammatory drug that is metabolised to its N-oxide by hFMO3 [15-17,21,25], tamoxifen, a breast cancer drug with antiestrogenic effect, also N-oxygenated by hFMO3 [15-17,21,26,27],and sulindac sulfide, a nonsteroidal anti-inflammatory drug [11] that is selectively re-oxidised to sulindac by hFMO3 S-oxygenation [2,25].

2. Materials and methods

2.1. Chemicals

All the chemical products were obtained in analytical grade and dissolved in ultrapure deionized water immediately before use: GO (concentration of 4 mg/mL in water) from Graphenea (Spain); DDAB, benzydamine (hydrochloride), benzydamine N-oxide (hydrogen maleate), tamoxifen, sulindac sulfide and sulindac from Sigma-Aldrich (Italy); tamoxifen N-oxide from Biozol (Germany).

2.2. Site-directed mutants of hFMO3

WT hFMO3 cloning was performed using pJL2 expression vector and XbaI and HindIII restriction enzymes, as formerly reported [2]. E158K and E308G polymorphic variants were obtained using QuikChange Site-Directed Mutagenesis Kit (Stratagene, Italy). The primers used were constructed as follows with the mutation site highlighted in bold:

E158K

Forward primer: 5′ C AAC CTA CCA AAA **AAG** TCC TTT CCA GGA C 3′

Reverse primer: 5′ G TCC TGG AAA GGA **TTC** TTT TGG TAG GTT G 3′

E308G

Forward primer: 5’ C GTG AAG GAA TTC ACA **GGG** ACC TCG GCC ATT TTT G 3’

Reverse primer: 5’ C AAA AAT GGC CGA GGT **CCC** TGT GAA TTC CTT CAC G 3’

DNA sequencing of the clone confirmed the presence of the mutation in the correct position.

2.3. Expression and purification of human FMO3

WT, E158K and E308G hFMO3 proteins were obtained by expression in *Escherichia coli* (JM109) cells and purification by applying the protocol already optimized for the wild type enzyme [2]. In particular, the proteins were extracted from cells membrane fractions and purified using nickel affinity chromatography. After the purification, proteins purity was checked by visualization in a 10% SDS-polyacrylamide gel stained with Coomassie Blue. hFMO3 enzymes concentration was estimated considering an FAD equimolar content, an extinction coefficient of 11,300 M^{-1} cm^{-1} at 450 nm and a molecular weight of 56 kDa [28].

2.4. FTIR spectroscopy

Infrared spectroscopy experiments on hFMO3 polymorphic variants were performed on gold-PET flat surface as protein support using the single reflection grazing angle attenuated total reflectance (GATR) tool (Harrick, USA) on a Bruker Model Tensor 27 FT-IR spectrometer (Bruker Instruments, USA) in nitrogen purged environment at room temperature. Protein samples were prepared by modifying gold-PET supports with 10 µL of 20 mM DDAB solution in chloroform plus 5 µL of GO water dispersion (1 mg/mL). After 10 minutes at 25°C, to allow solvent evaporation, the gold-PET surfaces were further modified by adding 5 µL of protein solution. Substrates were then kept overnight at 4°C before FTIR experiments. Wavenumber range of acquisition was from 4000 to 800 cm^{-1}; scan velocity and resolution were set at 10

kHz and 4 cm^{-1} respectively. Spectra were acquired in triplicates and averaged data, obtained using Opus software (Bruker Instruments, USA) were corrected by subtracting of the control spectra, obtained in the absence of protein. The obtained spectra were analysed by Fourier self-deconvolution (deconvolution factor 50, noise reduction factor 0.8) in order to investigate the composition of the amide I band in terms of number and location of single components. Afterwards, data analysis and curve fitting were carried out using PeakFit software (SPSS Inc., USA).

2.5. Electrode preparation

The preparation of glassy carbon electrodes was obtained as previously described [21]. In particular, 10 μL of 20 mM DDAB solution in chloroform or DDAB plus 5 μL of GO water dispersion (1 mg/mL) were deposited on the electrode surface and left 10 minutes at 25°C to permit evaporation of the solvent. The electrodes were further modified by adding 5 μL of purified WT hFMO3 solution (145 μM), E158K hFMO3 solution (121 μM) or E308G hFMO3 solution (43 μM) and kept at least 2 hours at 4°C for before any other experimental procedure.

2.6. Cyclic voltammetry and chronoamperometry

All electrochemistry procedures were developed on Autolab PGSTAT12 potentiostat controlled by GPES3 software (Ecochemie, The Netherlands). Electrochemical setup was composed by an electrolysis glass cell equipped with a platinum wire counter electrode, Ag/AgCl (3 M NaCl) reference electrode and 3 mm diameter glassy carbon working electrode (BASi, USA). Electrolysis buffer was 50 mM phosphate buffer pH 7.4 with the addition of 100 mM KCl as supporting electrolyte.

hFMO3 polymorphic variants were studied electrochemically by cyclic voltammetry, in presence and in absence of GO, at 25°C in absence of oxygen using a glovebox (Belle Technologies, UK). Cyclic voltammetry was performed using a potential range between +100 and -750 mV at increasing scan rates.

Electrocatalysis experiments on newly prepared hFMO3/DDAB/GO glassy carbon electrodes were carried out using chronoamperometry at an applied potential of -650 mV for 15 min in presence of rising concentrations of benzydamine, tamoxifen or sulindac sulphide substrates. In order to choose the correct electrocatalysis duration, a series of experiments was performed in the presence of saturating concentration of benzydamine (300 μM) and the amount of product, benzydamine N-oxide, was measured after 5, 10, 15 and 20 minutes (Figure S1). The amount of product formed increased linearly in this time period, for this reason a reaction time of 15 minutes was chosen for electrocatalysis experiments. The stability of electrochemical performance of both WT and polymorphic hFMO3 on DDAB/GO electrodes was also confirmed by cyclic voltammetry by performing scans at different times from 0 to 20 minutes (Figure S2).

Substrate permeation throughout enzyme layer and minimisation of mass transport control at the electrode was achieved by using glassy carbon rotating disk electrodes controlled by a BASi RDE-2 rotator system (BASi, USA) set at 200 rpm rotation speed. Electrocatalysis samples obtained by chronoamperometry were immediately subjected to HPLC separation and quantification. The quantification of metabolites was achieved using calibration curves obtained by the injection of standard solutions for benzydamine N-oxide, tamoxifen N-oxide and sulindac.

2.7. HPLC

Electrocatalysis products were detected and quantified by injecting samples in an HPLC system coupled with a diode array UV detector (Agilent-1200, Agilent technologies, USA) with a 4.6 x 150 mm, 5 μm Eclipse XDB-C18 column as stationary phase, as previously reported [17]. Benzydamine and benzydamine N-oxide were separated using the following procedure: 0-10 minutes, gradient elution of acetonitrile from 20% to 40% and 50 mM KH_2PO_4 from 80% to 60%; 10-12 minutes, isocratic elution of 40% acetonitrile and 60% 50 mM KH_2PO_4; 12

minutes-end of the run, gradient elution of acetonitrile from 40% to 60% and 50 mM KH_2PO_4 from 60% to 40%. The flow rate was 1 mL/min and detection wavelength was 308 nm. Retention times were 17.5 min for benzydamine N-oxide and 20 min and benzydamine.

Tamoxifen and tamoxifen N-oxide were eluted isocratically using a mobile phase composed by 82% methanol and 18% triethylamine (1%), at a flow rate of 0.8 mL/min. Detection wavelength was 278 nm. Retention times were 7 min for tamoxifen N-oxide and 15 min and tamoxifen.

Sulindac sulfide and sulindac were separated using using the following procedure: 0-6 minutes, isocratic elution of 30% acetonitrile and 70% 50 mM KH_2PO_4, flow rate 1.4 mL/min; 6-12 minutes, gradient elution of acetonitrile to 45% and 50 mM KH_2PO_4 to 55%, and to flow rate 1.6 mL/min; 8 minutes-end of the run, isocratic elution of 45% acetonitrile and 55% 50 mM KH_2PO_4, flow rate 1.6 mL/min. Detection wavelength was set at 360 nm. Retention times were 5.2 min and 16 min for sulindac sulfide and sulindac, respectively.

3. Results and Discussion

3.1. FTIR spectroscopy

The effect of hFMO3 polymorphism on the secondary structure of E158K and E308G variants in the presence of GO was studied by FTIR spectroscopy. There is currently no published crystal structure of the wild type hFMO3 protein but using FTIR spectroscopy one can compare the wild type secondary structure content with the two polymorphic variants. As previously reported for the WT protein [21], also here no effect on the IR spectral features was observed for the two hFMO3 polymorphic variants due to the presence of GO (data not shown).

Figure 1A shows the spectrum obtained for the WT hFMO3 enzyme compared to those of E158K and E308G variants. All spectra exhibit the characteristic features of protein IR spectra: amide I, II and III bands. Amide I band (~1650 cm^{-1}) is associated to stretching vibrational

transition of peptidic carbonyl group and in minor part of out-of-phase C-N stretching vibration [29]. In this region of the IR spectrum a series of signals rigorously correlated to protein secondary structures can be observed. Amide I band is the result of the merging of these bands and for this reason the deconvolution of amide I, together with the estimation of the contribution of each single signal to the amide I band, can give important details about protein secondary structure composition. Amide II band is detectable at around 1545 $cm^{-1}$and is due to the out-of-phase bending of the peptidic N-H bond and the stretching of the peptidic C-N bond. The peak at 1517 cm^{-1} is related to the stretching of C-C bond and the bending of C-H bond of side chain tyrosine residues [29]. Amide III band can be observed in the wavenumbers range of IR spectrum between 1200 and 1400 cm^{-1}. This signal is related to the in-phase combination of the bending of the peptidic N-H and C-N bonds [30].

"Here Figure 1"

All in all, the results of infrared spectroscopy do not seem to show major differences related to hFMO3 polymorphism. However, a proper investigation on the secondary structure composition of both E158K and E308G hFMO3 variants was achieved by analysing the composition of the amide I band of both IR spectra in its component bands after identification of their position through the peak deconvolution (Figures 1B and 1C). It is well established that the profile of the amide I band of proteins is typical of their secondary structure and that secondary structure composition can be predicted analysing the amide I band component bands by deconvolution.

Amide I components were then assigned to the related protein secondary structure [29,30] and their involvement to the polymorphic proteins secondary structure composition was calculated in percentage both for E158K and E308G hFMO3. Table 1 compares the secondary structure components of hFMO3 polymorphic variants with those previously measured for WT protein

[21]. The results obtained are very similar for what concerns peak positions, but the percentages of the different components show some differences. In particular, variant E308G seems to be structurally more similar to the WT, with only some small differences in the turns and unordered loops, while the E158K shows more significant differences also in the alpha helices and beta sheets. Based on these results, the E158K mutation seems to show slight structural differences compared to WT protein. However, since there is no published crystal structure for the WT protein as mentioned above, it is difficult to unequivocally confirm these observed differences.

"Here Table 1"

3.2. Direct electrochemistry of hFMO3 polymorphic variants

Cyclic voltammetry of hFMO3 polymorphic variants was performed both on DDAB and on DDAB/GO glassy carbon electrodes. Figure 2 shows the different steps involved in the preparation of the immobilised enzyme(s) on GO modified glassy carbon electrodes.

"Here Figure 2"

Figure 3 (A and B) shows the cyclic voltammograms of immobilised E158K and E308G hFMO3, in the presence and in the absence of GO. As already shown for the wild type protein [21], reduction/oxidation process was found electrochemically reversible for both hFMO3 variants. On control electrodes prepared without enzymes, no voltammetric peaks were observed (data not shown). Peak currents and scan rate values up to 120 mV s^{-1} were found linearly correlated (Figure 3, insets). Based on the postulated of Laviron's theory [31], this property is typical of electroactive species restricted in thin layer that are not controlled by passive diffusion events. A significant increase in the redox peak currents of the polymorphic variants was observed in presence of GO ($P < 0.001$) as also previously noted for WT protein

[21]. Since no voltammetric peaks were detected on control electrodes in the absence of protein, the increase in voltammetric peak current values can be ascribed to GO improvement on electron transfer properties rather than to an increase of the mass on the electrode. Redox features of both E158K and E308G hFMO3/DDAB/GO electrodes are summarised in Table 2 and compared to those of free FAD and WT protein.

"Here Figure 3"

As can be seen, the mean potential ($E_{1/2}$) of both polymorphic variants was shifted to more positive values compared to free FAD and WT enzyme. No statistical differences were observed between peak-to-peak separation values, meaning that hFMO3 polymorphic variants, like WT protein, are characterised by a quasi- reversible electron transfer redox system.

"Here Table 2"

The calculation of apparent surface coverage (Γ) was obtained by plotting the peak current versus the scan rate through Faraday's law for both hFMO3 variants. Electron transfer rate constant (k_s) was determined for both variants by plotting cathodic and anodic peak potentials versus the logarithm of the scan rate using Laviron's equations [31]. For these calculations, cyclic voltammetry experiments were performed in order to investigate irreversible electrochemistry of hFMO3 proteins using a scan rate ranging from 10 to 22 V s^{-1}. The k_s values were estimated by measuring the intercept of E plot versus the natural logarithm of scan rate (Figure S3) and were calculated to be 64.4 ± 8.5 s^{-1} for E158K hFMO3/DDAB/GO and 51.0 ± 8.3 s^{-1} for E308G hFMO3/DDAB/GO. A statistical improvement in the electron transfer rate expressed by the k_s value was found when comparing E158K variant to WT protein, while no significant differences were found between E308G variant and WT hFMO3.

3.3. Electrocatalytic activity of hFMO3 polymorphic variants

Catalytic activity of hFMO3 polymorphic variants on GO electrodes was examined and compared to WT protein using benzydamine and tamoxifen by performing chronoamperometry on glassy carbon rotating disk electrodes (Figure 4A and B). The ability of both WT and polymorphic hFMO3 proteins to use reducing equivalents delivered by electrode to drive substrate oxygenation was firstly investigated by cyclic voltammetry were catalytic currents in the presence of saturating concentrations of benzydamine were observed (Figure S4, supplementary information).

"Here Figure 4"

Additional experiments were also performed on WT, E158K and E308G hFMO3 variants using sulindacsulfide in order to estimate and compare the S-oxygenation activity of all the proteins on GO electrodes (Figure 5). Kinetic parameters for N-oxidation of benzydamine and tamoxifen and S-oxidation of sulindac sulphide were estimated by performing electrocatalysis followed by HPLC quantification of the products. The calculation of reaction rates was done through electrocatalysis product quantification after correction of each value by subtraction of the related controls (Figure 4 and 5). Control samples were prepared using hFMO3 previously treated at 98 °C for 30 min in order to obtain a complete denaturation of the protein.

"Here Figure 5"

Michaelis-Menten constant (K_M) and turnover number (k_{cat}) values were estimated for benzydamine and tamoxifen N-oxygenation and for sulindac sulfide S-oxygenation by plotting velocity curves with Michaelis-Menten equation and are summarised in Table 3. For benzydamine electrocatalysis, K_M values were 77.0 ± 9.3 μM and 52.2 ± 6.3 μM for E158K and E308G variants, respectively. When comparing these values with WT protein, a significant difference was found for E158K but not for E308G. The calculated k_{cat} values for benzydamine

electrocatalysis were 35.5 ± 1.6 min^{-1} and 54.4 ± 2.1 min^{-1} for E158K and E308G variants, respectively. The turnover number values of both variants were statistically lower than those of WT. In both cases, E158K and E308G mutations had a negative effect on benzydamine catalysis, but only in the case of E158K variant this corresponds to a reduction in substrate affinity.

For tamoxifen electrocatalysis, K_M values were 47.1 ± 9.0 μM and 4.6 ± 0.5 μM, respectively for E158K and E308G hFMO3 (Table 3). Again, while no differences were found between K_M values of WT and E308G variant for tamoxifen, a significant decrease in the enzyme affinity for tamoxifen was detected in the case of E158K variant. The calculated k_{cat} values for tamoxifen electrocatalysis were 12.1 ± 0.7 min^{-1} and 20.3 ± 0.5 min^{-1} for E158K and E308G variants, respectively. In this case, E158K showed lower catalytic activity towards tamoxifen while E308G had higher activity when compared to WT hFMO3.

For sulindac sulfide electrocatalysis, K_M values were 45.2 ± 7.0 μM, 53.2 ± 7.8 μM and 41.0 ± 9.9 μM, respectively for WT, E158K and E308G hFMO3. As can be seen, there were no significant differences when comparing these values and therefore it can be concluded that the single mutations have no effect on the affinity of resulting enzymes for this drug. The calculated k_{cat} values for sulindac sulfide electrocatalysis were 64.9 ± 2.7 min^{-1}, 80.3 ± 3.3 min^{-1} and 61.5 ± 3.9 min^{-1} for WT, E158K and E308G variants, respectively.E158K variant showed a slightly higher catalytic activity with respect to WT, highlighting the fact that E158K mutation could be unfavourable for N-oxygenation activity of hFMO3 but favourable forits S-oxygenation activity. As for E308G mutation, no differences were observed for either the S-oxidation activity of this variant or the N-oxidation activity with benzydamine compared to the WT. However, this mutation was relevant fortamoxifen metabolism where it demonstrated the highest k_{cat}.

In order to better visualize the electrocatalysis data of the comparison between the WT hFMO3 and its two variants, the catalytic efficiency (k_{cat}/K_M ratio) for each enzyme was calculated and the data are summarised in the Table 3 together with K_M and k_{cat} values.

"Here Table 3"

As can be seen in the Table 3, sulindac sulfide metabolism is not affected by any of the two polymorphisms (1.5 for the two mutants versus 1.4 for WT). Regarding benzydamine, E158K variant shows half the catalytic efficiency of the WT enzyme (0.5 versus 1.1) but most importantly, this polymorphism has an 11-fold lower catalytic efficiency in the presence of tamoxifen (0.3 versus 2.8). As a result, patients carrying this polymorphism would not metabolise tamoxifen as quickly as the patients carrying the WT hFMO3 gene and therefore might benefit from a different dose of this drug. The reverse effect was seen with the E308G variant where the catalytic efficiency is enhanced by a factor of around 1.5 (4.4 versus 2.8). In this case, patients with this polymorphism will metabolisethe drug faster than the WT individuals and therefore might require a higher dose of this drug to obtain the same therapeutic effect.

The results were also compared with previously published data on the activity of hFMO3 polymorphic variants. A general decrease in hFMO3 activity has been associated both to E158K and E308G allelic variants [32]. Regarding benzydamine N-oxygenation, an impairment of the enzyme activity was found for E158K variant [33,34] using recombinant protein expressed in *E. coli* or in baculovirus infected insect cells microsomes. A further impairment was also observed for E158K-E308G double mutant of hFMO3. In none of the cases this impairment corresponded to a decreased affinity for benzydamine. In the case of sulindac sulfide S-oxygenation, E158K and E308G polymorphisms have also been associated with a decreased hFMO3 activity [34,35]. Moreover, *in vivo* studies demonstrated that E158K

and E308G polymorphisms occur more frequently in familial adenomatous polyposis patients responding well to sulindac sulfide [36,37]. As for tamoxifen N-oxygenation, Krueger and colleagues showed an improvement of both enzyme affinity and activity due to E158K mutation using a recombinant system in baculovirus [27].

In general, there are only a handful of published data on the activity of hFMO3 polymorphic variants and in some cases as mentioned above, these data are not consistent. Our data support the overall decrease in the N-oxygenation activity of the E158K polymorphic variant similar to the published literature data however, we do not observe any differences with sulindac sulfide. Furthermore, for tamoxifen metabolism only data on the E158K polymorphism has been published but we see the same improvement also in the activity of E308G [27].

4. Conclusions

The effect of polymorphism on enzyme turnover efficiency in the presence of drugs is an essential issue to be tackled for human hepatic drug metabolising enzymesincluding hFMO3. The different polymorphic variants of hFMO3 have been frequently associated with the lower activity of this enzyme. Two common polymorphic variants of hFMO3, E158K and E308G, were expressed in bacteria and immobilised on glassy carbon electrodes in the presence of GO. Due to the attractive electrochemical and mechanical properties of GO, this nanomaterial has been extensively used as a high performance electrochemical transducer. The presence of GO in the electrochemical set up enhanced the signal of both E158K and E308G hFMO3 variants in cyclic voltammetry. For both polymorphic variants, a positive shift in the redox potential was observed when compared to the WT protein. The catalytic properties of E158K and E308G polymorphic variants were measured using three known substrates of hFMO3; benzydamine, tamoxifen and sulindac sulfide and, the results were compared to those obtained for the WT enzyme. In particular, E158K variant showed a significant impairment in its N-oxygenation activity, both in the presence of benzydamine and tamoxifen, whereas E308G variant had an

increased N-oxygenation activity with tamoxifen. Moreover, none of the two variants showed any differences in catalytic efficiency when S-oxygenation of sulindac sulfide was tested. The possible involvement of GO in the metabolic pattern observed for hFMO3 polymorphic variants with respect to the WT protein was mainly excluded due to experimental data related to the preservation of both the correct protein folding (by FTIR) and the measured redox potentials of WT and polymorphic variants of hFMO3. However, unequivocal exclusion of the GO effect needs further investigations.

Finally in this work, the unique features of GO were applied to the elucidation of the role of hFMO3 polymorphism in drug metabolism, confirming that DDAB/GO electrode systems can be suitable for this purpose. In future, this electrochemical set up can be further developed into a high throughput platform not only for fast and reliable screening of new chemical entities but also for deciphering the effect of polymorphisms on the metabolism of each new drug candidate. The results of such analyses might help adjust the dose of different prescribed drugs based on the genetic makeup of each patient and as a consequence, a step closer towards personalised medicine.

ACKNOWLEDGMENT

The authors wish to acknowledge financial support from the Progetto Ateneo-San Paolo 2012 (Italy).

References

[1] J.R. Cashman, Role of flavin-containing monooxygenase in drug development, Expert Opin. Drug Metab. Toxicol. 4 (2008) 1507-1521. DOI: 10.1517/17425250802522188.

[2] G. Catucci, A. Occhipinti, M. Maffei, G. Gilardi, S.J. Sadeghi, Effect of human flavin-containing monooxygenase 3 polymorphism on the metabolism of aurora kinase inhibitors, Int. J. Mol. Sci. 14 (2013) 2707-2716. DOI: 10.3390/ijms14022707.

[3] D.M. Ziegler, An overview of the mechanism, substrate specificities and structure of FMOs. Drug Metab. Rev. 34 (2002) 503-511. DOI:10.1081/DMR-120005650

[4] S.K. Krueger, D.E. Williams, Mammalian flavin-containing monooxygenases: structure/function, genetic polymorphisms and role in drug metabolism, Pharmacol. Ther. 106(3) (2005) 357-387. DOI: 10.1016/j.pharmthera.2005.01.001.

[5] S. Veeravalli, B.A. Omar, L. Houseman, M. Hancock, S.G.G. Malagon, F. Scott, A. Janmohamed, I.R. Phillips, E.A. Shephard, The phenotype of a flavin-containing monooyxgenase knockout mouse implicates the drug-metabolising enzyme FMO1 as a novel regulator of energy balance. Biochem. Pharmacol. 90 (2014), 88-95. DOI:10.1016/j.bcp.2014.04.007.

[6] S.G. Gonzalez-Malagon, A.N. Melidoni, D. Hernandez, B.A. Omar, L. Houseman, S. Veeravalli, F. Scott, D. Varshavi, J. Everett, Y. Tsuchiya, J.F. Timms, I.R. Phillips, E.A. Shephard, The phenotype of a knockout mouse identifies flavin-containing monooxygenase 5 (FMO5) as a regulator of metabolic ageing. Biochem. Pharmacol. 96 (2015), 267-277. DOI:10.1016/j.bcp.2015.05.013

[7] R.C. Schugar, J.M. Brown, Emerging roles of flavinmonooxygenase 3 in cholesterol metabolism and atherosclerosis. Curr. Opin. Lipidol. 26 (2015), 426-431. DOI:10.1097/MOL.0000000000000215.

[8] S.B. Koukouritaki, R.N. Hines, Flavin-containing monooxygenase genetic polymorphism: impact on chemical metabolism and drug development, Pharmacogenomics 6 (2005) 807-822. DOI: 10.2217/14622416.6.8.807.

[9] I.R. Phillips, A.A. Francois, E.A. Shephard, The flavin-containing monooxygenases (FMOs): genetic variation and its consequences for the metabolism of therapeutic drugs. Curr. Pharmacogen. 5 (2007) 292-313. DOI: 10.2174/157016007782793683.

[10] I.R. Phillips, E.A. Shephard, Flavin-containing monooxygenases: mutations, disease and drug response. Trends Pharmacol. Sci. 29(6) (2008) 294-301. DOI: 10.1016/j.tips.2008.03.004.

[11] C. Gao, G. Catucci, G. Di Nardo, G. Gilardi, S.J. Sadeghi, Human Flavin-containing monooxygenase 3: structural mapping of gene polymorphisms and insights into molecular basis of drug binding, Gene 593 (2016) 91-99. DOI: 10.1016/j.gene.2016.08.020.

[12] C.T. Dolphin, A. Janmohamed, R.L. Smith, E.A. Shephard, I.R. Phillips, Missense mutation in flavin-containing monooxygenase 3 gene, FMO3, underlies fish-odour syndrome, Nat. Genet. 17 (1997) 491-494. DOI: 10.1038/ng1297-491.

[13] E.P. Treacy, B.R. Akerman, L.M. Chow, R. Youil, C. Bibeau, J. Lin, A.G. Bruce, M. Knight, D.M. Danks, J.R. Cashman, S.M. Forrest, Mutations of the flavin-containing monooxygenase gene (FMO3) cause trimethylaminuria, a defect in detoxication, Hum. Mol. Genet. 7 (1998) 839-845. DOI: 10.1093/hmg/7.5.839.

[14] S.C. Mitchell, R.L. Smith, Trimethylaminuria: the fish malodor syndrome, Drug Metab. Dispos. 29 (2001) 517-521.

[15] S.J. Sadeghi, R. Meirinhos, G. Catucci, V.R. Dodhia, G. Di Nardo, G. Gilardi, Direct electrochemistry of drug metabolising hFMO3: Electrochemical turnover of

benzydamine and tamoxifen, J. Am. Chem. Soc. 132 (2010) 458-459. DOI: 10.1021/ja909261p.

[16] S. Castrignanò, S.J. Sadeghi, G. Gilardi, Electro-catalysis by immobilized humanflavin-containing monooxygenase isoform 3 (hFMO3), Anal. Bioanal. Chem. 398 (2010) 1403-1409. DOI: 10.1007/s00216-010-4014-z.

[17] S. Castrignanò, S.J. Sadeghi, G. Gilardi, Entrapment of human flavin-containing monooxygenase 3 in the presence of goldnanoparticles: TEM, FTIR and electrocatalysis, Biochim.Biophys. Acta 1820(12) (2012) 2072-2078. DOI: 10.1016/j.bbagen.2012.09.017.

[18] S. Castrignanò, F. Valetti, G. Gilardi, S.J. Sadeghi. Graphene oxide mediated electrochemistry of glucose oxidase on glassy carbon electrodes, Biotechnol. Appl. Biochem. 63(2) (2016) 157-162. DOI: 10.1002/bab.1392.

[19] C. Galande, W. Gao, A. Mathkar, A.M. Dattelbaum, T.N. Narayanan, A.D. Mohite, P.M. Ajayan, Science and engineering of graphene oxide, Part. Part. Syst. Charact. 31 (2014) 619-638.

[20] D.R. Dreyer, A.D. Todd, C.W. Bielawski, Harnessing the chemistry of graphene oxide, Chem. Soc. Rev. 43 (2014) 5288-5301. DOI: 10.1002/ppsc.201300232.

[21] S. Castrignanò, G. Gilardi, S.J. Sadeghi, Human flavin-containing monooxygenase 3 on graphene oxide for drug metabolism screening, Anal. Chem. 87(5) (2015) 2974-2980. DOI: 10.1021/ac504535y.

[22] M. Pumera, Graphene in biosensing, Mater. Today 14 (2011) 308-315. DOI: 10.1016/S1369-7021(11)70160-2.

[23] M.S. Artiles, C.S. Rout, T.S. Fisher, Graphene-based hybrid materials and devices for biosensing, Adv. Drug Deliv. Rev. 63 (2011) 1352-1360. DOI: 10.1016/j.addr.2011.07.005.

[24] T. Kuila, S. Bose, P. Khanra, A.K. Mishra, N.H. Kim, J.H. Lee, Recent advances in graphene-based biosensors, Biosens. Bioelectron. 26 (2011) 4637-4648. DOI:10.1016/j.bios.2011.05.039.

[25] M.A. Hamman, B.D. Haehner-Daniels, S.A. Wrighton, A.E. Rettie, S.D. Hall, Stereoselective sulfoxidation of sulindac sulfide by flavin-containing monooxygenases, Biochem. Pharmacol. 60 (2000) 7-17. DOI: 10.1016/S0006-2952(00)00301-4.

[26] E. Hodgson, R.L. Rose, Y. Cao, S.S. Dehal, D. Kupfer, Flavin-containing monooxygenase isoform specificity for the N-oxidation of tamoxifen determined by product measurement and NADPH oxidation, J. Biochem. Mol. Toxicol. 14 (2000) 118-120. DOI: 10.1002/(SICI)1099-0461(2000)14:2<118::AID-JBT8>3.0.CO;2-T.

[27] S.K. Krueger, J.E. Vandyke, D.E. Williams, R.N. Hines, The role of flavin-containing monooxygenase (FMO) in the metabolism of tamoxifen and other tertiary amines, Drug Metab. Rev. 38 (2006) 139-147. DOI: 10.1080/03602530600569919.

[28] G. Catucci, G. Gilardi, L. Jeuken, S.J. Sadeghi, In vitro drug metabolism by C-terminally truncated human flavin-containing monooxygenase 3, Biochem. Pharm. 83 (2012), 551-558. DOI: 10.1016/j.bcp.2011.11.029

[29] Barth, C.Q. Zscherp, What vibrations tell us about proteins, Rev. Biophys. 35 (2002) 369-430. DOI: 10.1017/S0033583502003815.

[30] Barth, Infrared spectroscopy of proteins, Biochim. Biophys. Acta 1767 (2007) 1073-1101. DOI: 10.1016/j.bbabio.2007.06.004.

[31] E. Laviron, General expression of the linear potential sweep voltammogram in the case of diffusionless electrochemical systems, J. Electroanal. Chem. 101 (1979) 19-28. DOI: 10.1016/S0022-0728(79)80075-3.

[32] J.R. Cashman, B.R. Akerman, S.M. Forrest, E.P Treacy, Population-specific polymorphisms of the human FMO3 gene: significance for detoxication, Drug Metab.Dispos. 28(2) (2000) 169-173.

[33] E. Störmer, I. Roots, J. Brockmöller, Benzydamine N-oxidation as an index reaction reflecting FMO activity in human liver microsomes and impact of FMO3 polymorphisms on enzyme activity, Br. J.Clin. Pharmacol. 50(6) (2000) 553-561. DOI: 10.1046/j.1365-2125.2000.00296.x.

[34] M. Shimizu, H. Yano, S. Nagashima, N. Murayama, J. Zhang, J.R. Cashman, H. Yamazaki, Effect of genetic variants of the human flavin-containing monooxygenase 3 on N- and S-oxygenation activities, Drug Metab. Dispos. 35(3) (2007) 328-330. DOI: 10.1124/dmd.106.013094.

[35] H. Yamazaki, M. Shimizu, Survey of variants of human flavin-containing monooxygenase 3 (FMO3) and their drug oxidation activities, Biochem. Pharmacol. 85(11) (2013) 1588-1593. DOI: 10.1016/j.bcp.2013.03.020.

[36] I.M. Hisamuddin, M.A. Wehbi, A. Chao, H.W. Wyre, L.M. Hylind, F.M. Giardiello, V.W. Yang, Genetic polymorphisms of human flavin monooxygenase 3 in sulindac-mediated primary chemoprevention of familial adenomatous polyposis, Clin. Cancer Res. 10(24) (2004) 8357-8362. DOI: 10.1158/1078-0432.CCR-04-1073.

[37] I.M. Hisamuddin, M.A. Wehbi, B. Schmotzer, K.A. Easley, L.M. Hylind, F.M. Giardiello, V.W. Yang, Genetic polymorphisms of flavin monooxygenase 3 in sulindac-induced regression of colorectal adenomas in familial adenomatous polyposis,

Cancer Epidemiol. Biomarkers Prev. 14(10) (2005) 2366-2369. DOI: 10.1158/1055-9965.EPI-05-0312.

Table 1: Secondary structure content calculation from the deconvolution of the Amide I band of FTIR spectra.

Structure	WT hFMO3/DDAB/GO[1]		E158K hFMO3/DDAB/GO		E308G hFMO3/DDAB/GO	
	Peak position	**Area**	**Peak position**	**Area**	**Peak position**	**Area**
α helix	1657 cm^{-1} 1666 cm^{-1}	34 %	1658 cm^{-1} 1667 cm^{-1}	30 %	1659 cm^{-1} 1667 cm^{-1}	34 %
β sheet	1629 cm^{-1}	21 %	1632 cm^{-1}	25 %	1632 cm^{-1}	22 %
Turn	1676 cm^{-1} 1688 cm^{-1}	24 %	1675 cm^{-1} 1683 cm^{-1}	17 %	1675 cm^{-1} 1686 cm^{-1}	20 %
Unordered	1647 cm^{-1}	21 %	1647 cm^{-1}	28%	1648 cm^{-1}	24 %

[1]Previously published results [21].

Table 2: Redox properties of hFMO3 polymorphic variants in the presence of GO compared to those of free FAD and WT protein.

	$E_{1/2}$ / mV	ΔE / mV	Γ / pmol cm^{-2}	k_s / s^{-1}
FAD[1]	-344 ± 4	49 ± 1	65 ± 7	n.d.
WT[1]	-357 ± 3*	60 ± 5	32 ± 2	48.1 ± 3.0
E158K	-298 ± 4*,##	60 ± 4	22 ± 2	64.4 ± 8.5 #
E308G	-298 ± 1*,##	62 ± 6	9 ± 0.0	51.0 ± 8.3

One way ANOVA followed by Student-Newman-Keuls post hoc test: * $P < 0.001$ compared to FAD; # $P < 0.05$, ## $P < 0.001$ compared to WT.[1]Previously published results [21].

Table 3: Summary of kinetic parameters of hFMO3 WT and its polymorphic variants with the three tested drugs using GO modified glassy carbon electrodes.

	Benzydamine			**Tamoxifen**			**Sulindac Sulfide**		
	K_M / µM	**k_{cat} / min^{-1}**	**k_{cat}/K_M**	**K_M / µM**	**k_{cat} / min^{-1}**	**k_{cat}/K_M**	**K_M / µM**	**k_{cat} / min^{-1}**	**k_{cat}/K_M**
WT	58.9 ± 9.1[1]	63.2 ± 2.2[1]	1.1 ± 0.2	5.8 ± 1.1[1]	16.4 ± 0.6[1]	2.8 ± 0.6	45.2 ± 7.0	64.9 ± 2.7	1.4 ± 0.2
E158K	77.0 ± 9.3[*]	35.5 ± 1.6[§]	0.5 ± 0.1[§]	47.1 ± 9.0[§]	12.1 ± 0.7[§]	0.3 ± 0.1[§]	53.2 ± 7.8	80.3 ± 3.3[#]	1.5 ± 0.2
E308G	52.2 ± 6.3	54.4 ± 2.1[§]	1.0 ± 0.1	4.6 ± 0.5	20.3 ± 0.5[§]	4.4 ± 0.5[#]	41.0 ± 9.9	61.5 ± 3.9	1.5 ± 0.4

One-way ANOVA followed by Student-Newman-Keuls post hoc test: * $P < 0.05$, [#] $P < 0.01$, [§] $P < 0.001$ compared to WT hFMO3/DDAB/GO. [1]Previously published results [21].

FIGURE LEGENDS

Figure 1: A) FTIR spectra of WT (1), E158K (2) and E308G (3) hFMO3 protein in the presence of graphene oxide. Amide I band with individual components fitted for E158K hFMO3 (B) and E308G hFMO3(C)in the presence of graphene oxide.

Figure 2: Schematic representation of the different steps involved in the preparation of the immobilised hFMO3 enzyme(s) on graphene oxide modified glassy carbon electrodes.

Figure 3: Cyclic voltammograms of E158K (A) and E308G (B) hFMO3 on DDAB glassy carbon electrodes in the absence (dashed line) and in the presence (solid line) of graphene oxide presented without baseline correction (lower graph) and with baseline correction (upper graph) obtained by subtraction of hFMO3 from control electrodes. Scan rate: 120 mV s^{-1}. Insets: plot of cathodic (filled symbols) and anodic (empty symbols) peak currents versus scan rate for hFMO3 on DDAB glassy carbon electrodes in the absence (triangles) and in the presence (circles) of graphene oxide. R^2>0.99.

Figure 4: Electrocatalytically produced benzydamine N-oxide (A) and tamoxifen N-oxide (B) by WT (black circles), E158K (black squares) and E308G (white triangles) hFMO3/DDAB/GO glassy carbon electrodes: plot of reaction velocity versus substrate concentration fitted to Michaelis-Menten equation. Data are shown as mean ± SD of at least three different electrode measurements. WT published results [21] added for direct comparison.

Figure 5: Electrocatalytically produced sulindac sulfoxide by WT (filled circles), E158K (black squares) and E308G (empty triangles) hFMO3/DDAB/GO glassy carbon electrodes:

plot of reaction velocity versus substrate concentration fitted to Michaelis-Menten equation. Data are shown as mean ± SD of at least three different electrode measurements.

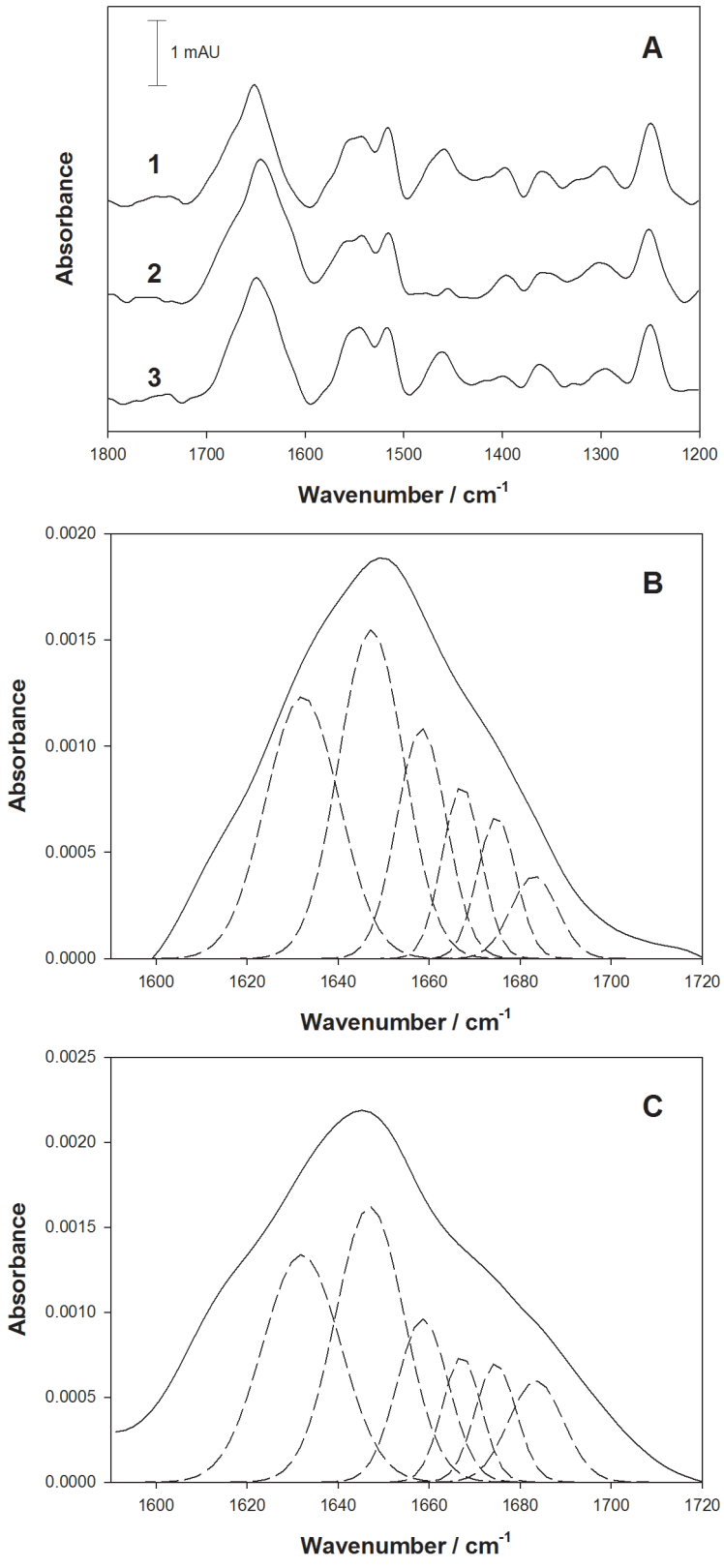
A
1 mAU
1
2
3
Absorbance
1800
1700
1600
1500
1400
1300
1200
Wavenumber / cm-1
B
0.0020
0.0015
0.0010
0.0005
0.0000
Absorbance
1600
1620
1640
1660
1680
1700
1720
Wavenumber / cm-1
C
0.0025
0.0020
0.0015
0.0010
0.0005
0.0000
Absorbance
1600
1620
1640
1660
1680
1700
1720
Wavenumber / cm-1

FIGURE 1

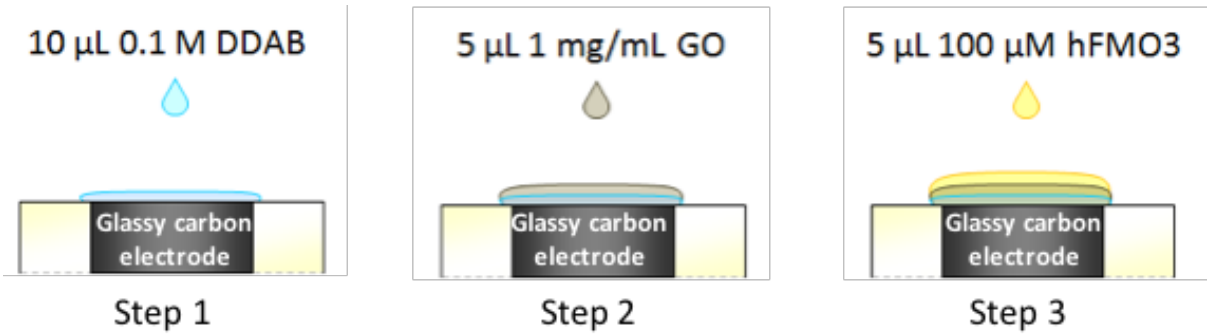
10 µL 0.1 M DDAB
Glassy carbon electrode
Step 1
5 µL 1 mg/mL GO
Glassy carbon electrode
Step 2
5 µL 100 µM hFMO3
Glassy carbon electrode
Step 3

FIGURE 2

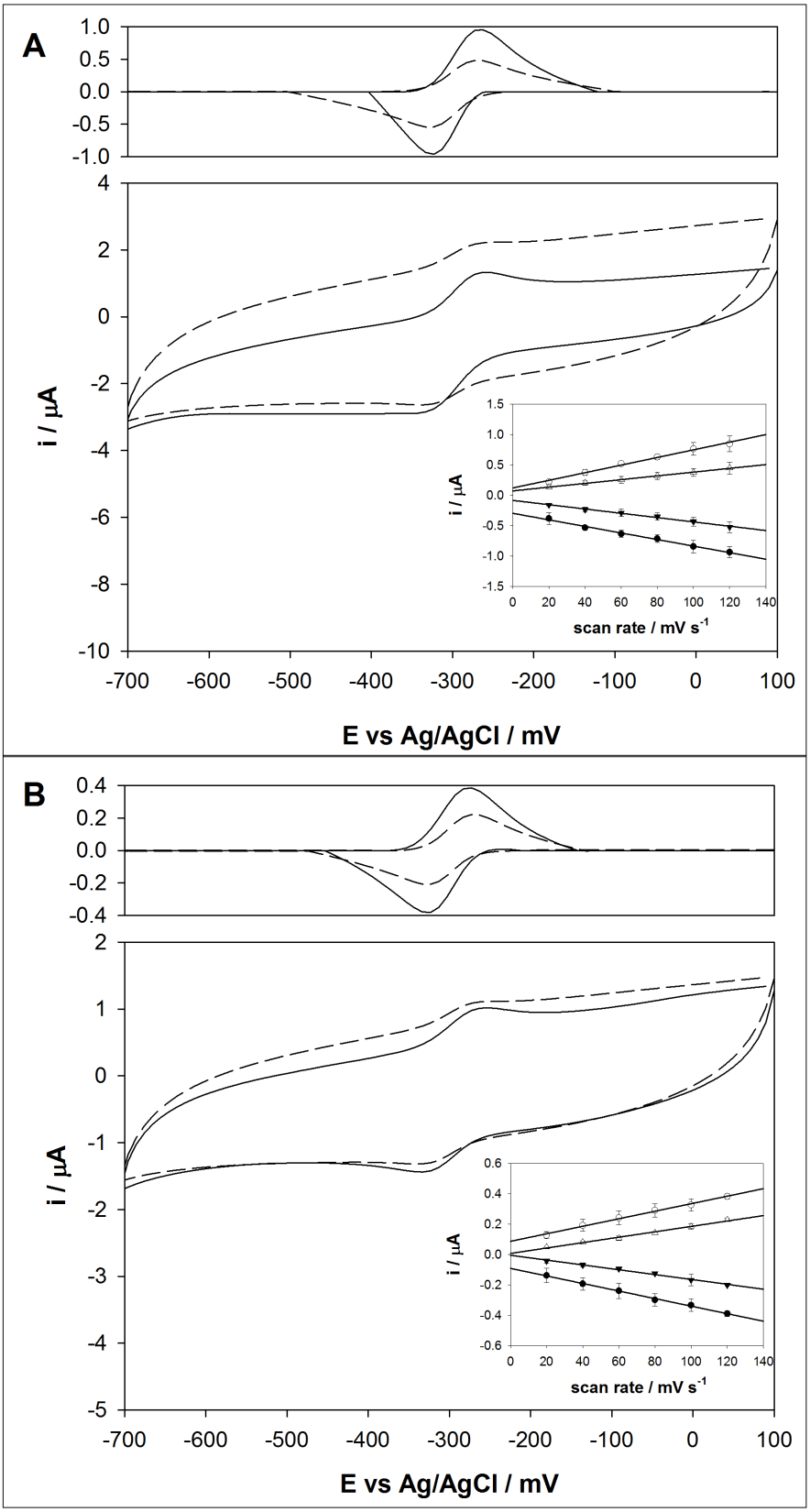
A
1.0
0.5
0.0
-0.5
-1.0
4
2
0
-2
-4
-6
-8
-10
i / µA
-700
-600
-500
-400
-300
-200
-100
0
100
E vs Ag/AgCl / mV
1.5
1.0
0.5
0.0
-0.5
-1.0
-1.5
i / µA
0
20
40
60
80
100
120
140
scan rate / mV s-1
B
0.4
0.2
0.0
-0.2
-0.4
2
1
0
-1
-2
-3
-4
-5
i / µA
-700
-600
-500
-400
-300
-200
-100
0
100
E vs Ag/AgCl / mV
0.6
0.4
0.2
0.0
-0.2
-0.4
-0.6
i / µA
0
20
40
60
80
100
120
140
scan rate / mV s-1

FIGURE 3

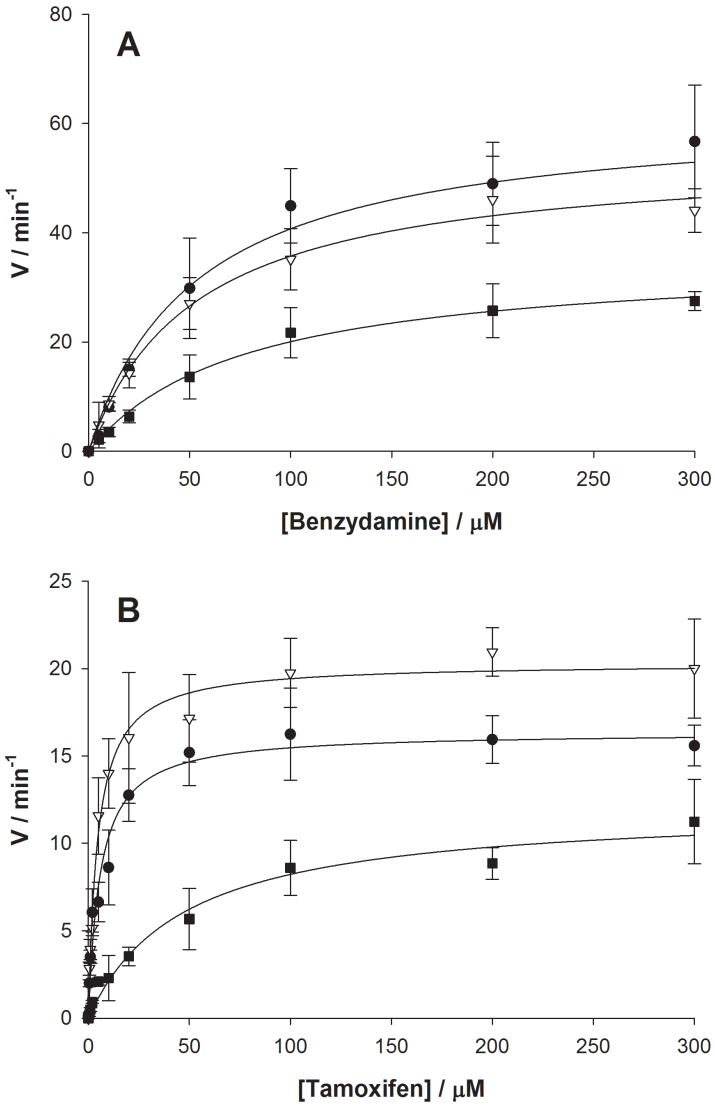
A
V / min-1
80
60
40
20
0
0
50
100
150
200
250
300
[Benzydamine] / μM
B
V / min-1
25
20
15
10
5
0
0
50
100
150
200
250
300
[Tamoxifen] / μM

FIGURE 4

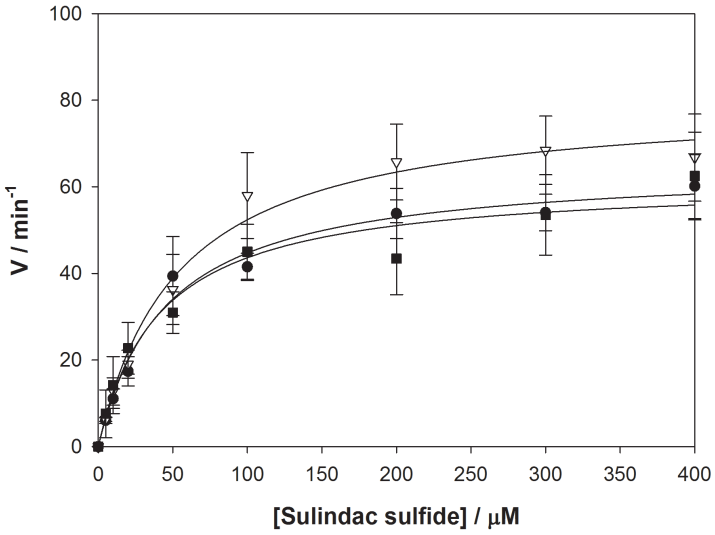
100
80
60
40
20
0
V / min-1
0
50
100
150
200
250
300
350
400
[Sulindac sulfide] / μM

FIGURE 5